Measuring the decoherence of a quantronium qubit with the cavity bifurcation amplifier

M. Metcalfe, E. Boaknin, V. Manucharyan, R. Vijay, I. Siddiqi, C. Rigetti, L. Frunzio, R. J. Schoelkopf, and M. H. Devoret
Department of Physics and Applied Physics, Yale University, New Haven, Connecticut, USA 06520–8284
(Received 7 June 2007; revised manuscript received 19 September 2007; published 21 November 2007)

Dispersive readouts for superconducting qubits have the advantage of speed and minimal invasiveness. We have developed such an amplifier, the cavity bifurcation amplifier (CBA), and applied it to the readout of the quantronium qubit. It consists of a Josephson junction embedded in a microwave on-chip resonator. In contrast with the Josephson bifurcation amplifier, which has an on-chip capacitor shunting a junction, the resonator is based on a simple coplanar waveguide imposing a predetermined frequency and whose other rf characteristics such as the quality factor are easily controlled and optimized. Under proper microwave irradiation conditions, the CBA has two metastable states. Which state is adopted by the CBA depends on the state of a quantronium qubit coupled to the CBA's junction. Due to the megahertz repetition rate and large signal to noise ratio, we can show directly that the coherence is limited by $1/f$ gate charge noise when biased at the "sweet spot"—a point insensitive to first order gate charge fluctuations. This architecture lends itself to scalable quantum computing using a multiresonator chip with multiplexed readouts.

DOI: 10.1103/PhysRevB.76.174516 PACS number(s): 85.25.Cp, 03.67.Lx, 74.50.+r

INTRODUCTION

Quantum circuits based on Josephson junctions[1] are candidates for the fundamental building block of a quantum computer—a quantum bit, or qubit. Several implementations have been tested,[2–8] which may be distinguished by the variable controlling the state of the qubit (charge, flux, or phase) and the technique used for the readout. These systems can be individually addressed, controlled, and read, making them some of the most advanced solid state qubits.

An enabling characteristic of many superconducting qubits is the existence of an optimal bias point where the qubit is immune to first order to fluctuations in external control parameters. Nonetheless, even systems operated at this "sweet spot" have coherence times limited by second order fluctuations of the external control parameters.[9] In this paper we describe measurements of a quantronium qubit operated at this optimal bias point[2,8] employing the recently developed cavity bifurcation amplifier (CBA)—a fast, dispersive, scalable readout system based on a driven nonlinear superconducting resonator.[10,11] With this architecture, we can measure the fluctuations in the quantronium's coherence on time scales as short as a second, allowing us to probe the $1/f$ property of charge noise on these scales. These measurements confirm previous studies of the limitations of coherence times in charge qubits[9,12] and cast additional light on the fluctuating character of T_2 itself and how its value depends on the measurement protocol.

The nonlinearity of the CBA is provided by a Josephson junction placed in the center of a $\lambda/2$ on-chip coplanar waveguide resonator with both an input and an output coupling capacitor playing the role of Fabry-Pérot cavity mirrors (see Fig. 1). When driven with a microwave signal at frequency ν_d such that $\nu_d < \nu_0(1-\sqrt{3}/Q)$, where ν_0 is the resonator small oscillation natural frequency and Q the loaded quality factor, this system can have two dynamical metastable states which differ by their oscillation amplitude and phase. As the driving power P is ramped past the bifurcation power P_b, the CBA switches from the state of low amplitude to the state with high amplitude. We detect the state of the nonlinear oscillator by monitoring the amplitude and phase change of the microwave signal transmitted by the resonator. In parallel with the CBA's junction, we place a split Cooper pair box (SCPB), a circuit known as the quantronium, giving the resonator two bifurcation powers $P_b^{|0\rangle}$ and $P_b^{|1\rangle} < P_b^{|0\rangle}$ depending on the state of the qubit, $|0\rangle$ or $|1\rangle$. The two qubit states are mapped into the two metastable states of the CBA by ramping quickly the power P to a level intermediate between $P_b^{|0\rangle}$ and $P_b^{|1\rangle}$. If the quantronium qubit is in $|1\rangle$, the CBA will switch to the high oscillating state, whereas if it is in $|0\rangle$, the CBA will remain in the low oscillating state.

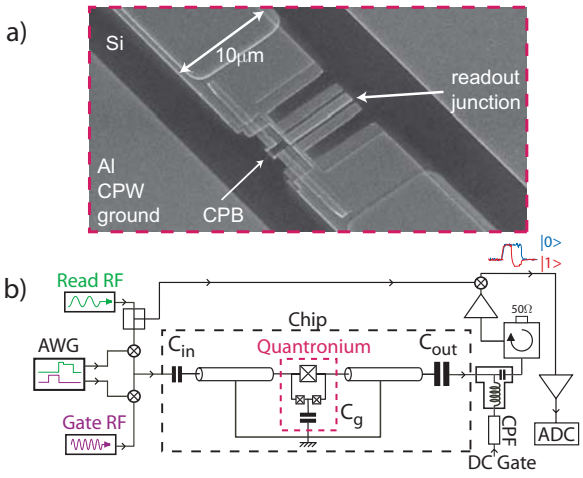

FIG. 1. (Color online) (a) Scanning electron micrograph of a duplicate of the measured device, both of which are fabricated on the same chip simultaneously. (b) Schematic of our sample and its environment. The sample consists of a split Cooper pair box whose loop is interrupted with a large junction (quantronium). The state of the quantronium alters the switching probability P_{01} of the CBA between its two metastable states, which can be inferred from the amplitude and phase change of transmitted microwave pulses through the device.

This readout has the advantage of being nondissipative as the readout junction never switches into the normal state, unlike the original dc-biased quantronium readout.[2] This dispersive readout minimally disturbs the qubit state and since after switching we do not need to wait for quasiparticles to relax, the repetition rate is only limited by the relaxation time T_1 of our qubit and the Q of our resonator. Like the dc readout, the CBA readout can latch,[13] allowing enough time for the measurement of the complex amplitude of the transmitted wave and therefore excellent signal to noise ratio. These characteristics were also present in the Josephson bifurcation amplifier,[8,13,14] which implemented a bifurcating nonlinear oscillator using a lumped element capacitor in parallel with the junction. However this capacitor was fabricated using a $Cu/Si_3N_4/Al$ multilayer structure, which was difficult to fabricate and integrate with more than one qubit. Also, the parallel plate geometry suffered from inherent stray inductive elements. In contrast, the CBA is fabricated using a simple coplanar waveguide (CPW) geometry with no stray elements. The resonance frequency ν_0 and the quality factor Q are controlled by the resonator length and output capacitor, respectively. The CBA geometry thus offers the possibility of designing a multiresonator chip with multiplexed readouts, which would accommodate up to ten qubits at once, an important step toward scalable quantum computing. The present work, in addition to the assessment of $1/f$ noise in a new architecture, is a first step in this direction.

SAMPLE FABRICATION AND CHARACTERIZATION

The resonator is initially fabricated using photolithography on a bare Si wafer.[15] A LOR5A/S1813 optical resist bilayer is used and the development is optimized to have at least 50 nm of undercut beneath the S1813 to avoid wavy edges and to obtain a sloped edge on the resonator. This sloped edge is obtained by evaporating a 200 nm thick Al layer onto the sample at 0.2 nm/s with an angle of 5° and with a stage rotation of 10°/s. Next, the quantronium is fabricated using electron beam lithography. We use a MMA/PMMA resist bilayer and the Dolan bridge double angle evaporation technique to fabricate our junctions.[16] For this sample, the split Cooper pair box is fabricated first inside the resonator, followed by the readout junction in a separate step using a new e-beam resist. Using a hollow cathode Ar ion gun, we obtain an Ohmic contact between the two e-beam layers and the resonator.

For the qubit sample described in this paper, we have been working with a linear regime resonance frequency $\nu_0 = 9.64$ GHz and a Q of 160. An on-chip twin [Fig. 1(a)] of the SCPB of the quantronium had a normal state resistance of 15 kΩ, with small junction areas of 0.05 μm^2. The usual gate line of the quantronium is absent in our design since we use the readout lines to access both the rf and dc gate lines, another advantage of this configuration.

QUBIT CHARACTERIZATION

We performed gate charge and flux modulations while keeping the qubit in its ground state, to check that we have

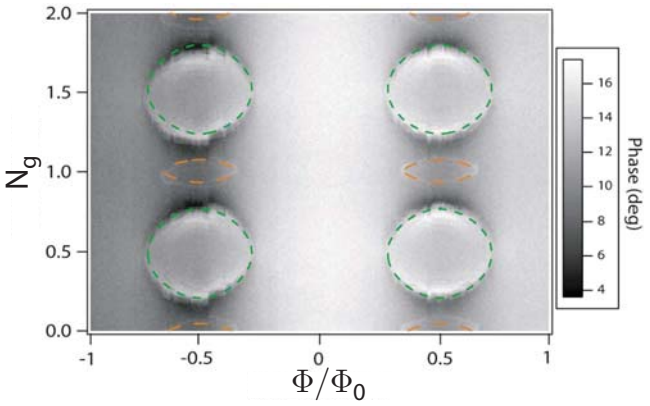

FIG. 2. (Color online) Gate charge and flux modulations of our device. We operated in the weakly nonlinear mode ($P \ll P_b^{|1\rangle}$) and monitored the phase of the transmitted signal (grayscale) as we varied the applied gate charge $N_g = C_g V_g / 2e$ and flux Φ ($\Phi_0 = \hbar/2e$). The large ellipsoidal contours can be interpreted as induced transitions between the energy levels of the qubit at multiples of the readout frequency. The green fitted lines are transitions between the 0 and 1 energy levels at the readout frequency of 9.64 GHz, while the orange fits are for transitions between the 0 and 2 energy levels at twice the readout frequency, 19.28 GHz.

flux periodicity and $2e$ charge periodicity, as shown in Fig. 2. The readout was first operated in the weakly nonlinear mode ($P \ll P_b^{|1\rangle}$) and we measured changes in the phase of the transmitted signal as the gate charge and flux were varied, keeping the frequency fixed at the maximal phase response point (see Fig. 2). Apart from a slow background modulation due to the changing susceptibility of the ground state, we observe sharp contrast on contours of ellipsoidal shape. These can be interpreted as contours of constant qubit transition frequency coinciding with the readout frequency or its double, an effect similar to that observed by Wallraff *et al.*[6] Using the well known expressions for the energy levels of the quantronium,[17] we can reproduce the shape of these contours, within the uncertainty due to the low frequency gate charge and flux noises, and extract a Jospehson energy of the SCPB E_J of 15 GHz and charging energy $E_{CP} = (2e)^2/2C_\Sigma$ of 17 GHz, where C_Σ is the sum of the capacitances of the junctions in the SCPB and the gate capacitance.

To get a more precise measurement of E_J and E_{CP}, we performed spectroscopy on the qubit by applying a weakly exciting 1 μs long pulse, followed by a latching readout pulse. The switching probability P_{01} between the two metastable states of the CBA is measured as the spectroscopic frequency ν_s is swept for each gate charge step, at zero flux. Due to the cross-talk between the readout and the qubit, we have to ensure that we have zero leakage of spectroscopic power outside our pulse. This is achieved by gating the LO on the mixers shaping our pulses, with a pulse shape which is a few nanoseconds longer than the spectroscopic pulse. As a function of frequency, we find a peak in the switching probability, whose position varies with gate charge with the expected sinusoidal-like shape shown in Fig. 3. The theoretical fit, shown in red, refines the previous determination of E_J and E_{CP} to the values $E_J = 15.02$ GHz and E_{CP}

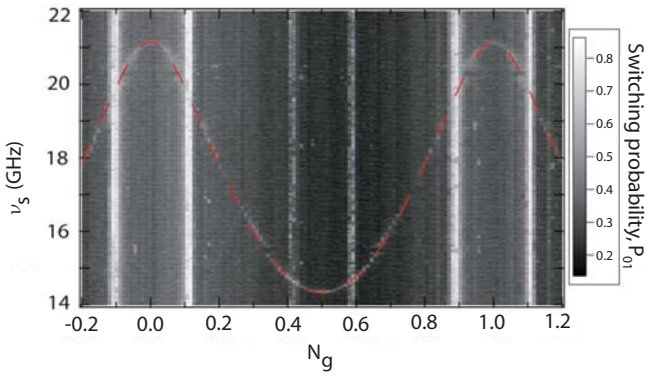

FIG. 3. (Color online) Spectroscopy peak as a function of gate charge N_g. Staying at zero flux, we measure P_{01} while sweeping ν_s and stepping N_g. The theoretical fit of the resulting sinusoidal-like dependence of the peak with N_g is given by the red dashed line with the fit parameters E_J=15.02 GHz and E_{CP}=17.00 GHz. The vertical lines with no N_g dependence are the excitations between qubit energy levels enduced at multiples of the readout frequency, similar to those seen in Fig. 2.

=17.00 GHz. Zooming in to the double sweet spot, N_g=0.5, Φ/Φ_0=0, where the qubit is immune to charge and flux noise to first order, we measure a Lorentzian spectroscopic peak of width $\Delta\nu_{01}$=2.6 MHz and a Larmor frequency ν_{01} =14.35 GHz. This gives a dephasing time, $T_2=1/\pi\Delta\nu_{01}$, of 120 ns. However, large charge jumps move the biasing point off the sweet spot causing the linewidth to be widened. More accurate measurements of T_2 will be obtained from Ramsey fringes where we can follow the variation of T_2 with time.

QUBIT MANIPULATION AND COHERENCE EXPERIMENTS

Once the qubit parameters are known, we can perform experiments on the qubit to determine the qubit's quality in terms of its energy relaxation time T_1 and dephasing time T_2. An essential part of these experiments is the need to control the state of the qubit precisely. This is achieved by applying a microwave pulse to the gate with rectangular envelope of amplitude A and time length τ. In a frame rotating at the gate pulse carrier frequency ν_s, the qubit state then precesses at a frequency, ν_p, given by[17]

$$\nu_p = [(\nu_{Rabi})^2 + (\nu_{01} - \nu_s)^2]^{1/2}, \quad (1)$$

where the Rabi frequency[18] $\nu_{Rabi}=2E_{CP}\Delta N_g\langle 0|N|1\rangle/h$ involves the gate modulation amplitude in units of Cooper pairs $\Delta N_g=C_gA/2e$ and charge operator matrix element between the excited and ground states $\langle 0|N|1\rangle$. For A=0, we have free evolution at the Ramsey frequency[19] $\nu_{Ramsey}=|\nu_{01} - \nu_s|$.

We begin by measuring the Rabi oscillations. The pulse sequence protocol involves a gate pulse with fixed $\nu_s=\nu_{01}$ and varying amplitude A and time length τ, followed by a latching readout pulse. The sequence is repeated 10^4 times to measure the switching probability. The oscillations of the switching probability as a function of τ and A are plotted in

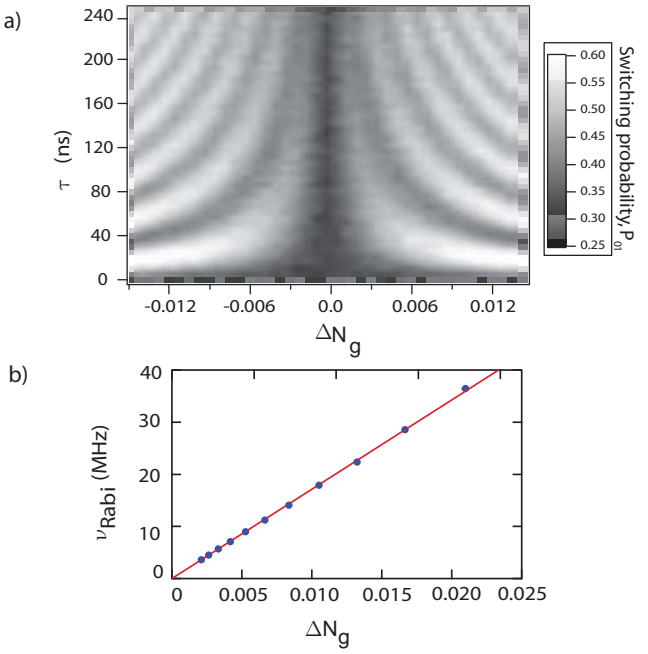

FIG. 4. (Color online) (a) Rabi oscillations in the switching probability P_{01}, as a function of gate charge modulation ΔN_g and gate pulse time length τ. ΔN_g is calculated from the Rabi pulse envelope voltage A reaching the sample through the attentuation in the input lines and is plotted in terms of Cooper pairs, $\Delta N_g = C_gA/2e$. Oscillations in the switching probability P_{01} are seen with both ΔN_g and τ. (b) Fitted Rabi frequency ν_{Rabi} vs ΔN_g. As expected from a two-level system, ν_{Rabi} scales linearly with ΔN_g.

Fig. 4. The extracted frequency ν_{Rabi} scales linearly with ΔN_g [Fig. 4(b)] as expected from a two-level system. From the position of the first maximum of the Rabi oscillations, we can calibrate the pulse time length needed for a π pulse, which drives the qubit from the ground state to the excited state. Using this π pulse, we measure the exponential decay of the population of the excited state (data not shown) and obtain the relaxation time T_1 which, during the course of an experimental run, varied between 1.4 and 1.8 μs, with a persistence time of a few seconds. These values are comparable to the results of Vion *et al.*[2] and Siddiqi *et al.*[8]

The maximum contrast measured is about 60%, lower than the maximum contrast of over 99.9%, calculated for the ideal case of a nonrelaxing qubit given the measured parameters of the resonator. This loss can be attributed to three main sources. First, the qubit relaxes before the readout takes place because of its finite T_1, resulting in a 10% loss in contrast. Second, the qubit relaxes to the ground state as the readout voltage approaches the bifurcation voltage, resulting in a further 25% loss in contrast. Other measurements (not described here) have suggested that this loss in contrast could be from Stark shifting the qubit to lower frequencies during readout, where it can come in resonance with spurious transitions,[20] possibly due to defects in the substrate or in the tunnel barrier. The remaining loss could be accounted for by the fact that the transition between the two oscillating states of the CBA is broadened by more than a factor of 5 from that expected.

To measure the coherence time, T_2, we follow a different pulse protocol in which we apply two $\pi/2$ pulses separated

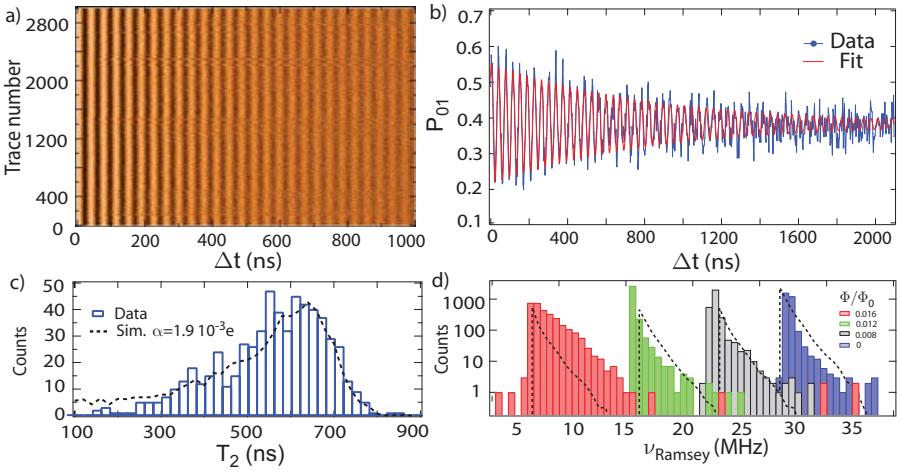

FIG. 5. (Color online) (a) 3000 Ramsey oscillations as a function of free evolution time Δt. Each trace is 2.1 μs long with 3 ns per step. They each take 0.35 s to acquire. We can see visually the variation of T_2 for the different Ramsey fringes by noticing the variation in contrast in the fringes near 1 μs. (b) Sample data fit. We average five of the acquired Ramsey traces shown in (a) and fit to a decaying sinusoid to extract the T_2 which is then plotted in (c). For this particular case, we have a coherence time of 840 ns and a Ramsey frequency of 26.9 MHz. (c) Distribution of T_2 for 3000 of the Ramsey traces (600 fits). The black dashed line is the result of a simulation of the free evolution decay of the Ramsey fringes with $1/f$ noise fluctuations on the gate, $S_q(\omega)=\alpha^2/|\omega|$. In the simulation, we used ten times more points compared to the data to obtain a smoother curve. (d) Corresponding distribution of Ramsey frequencies at four different flux biasing points. Each distribution has 3000 Ramsey traces. The blue histogram corresponds to the data in (a), (b), and (c). The Ramsey frequency is extracted from the position of the maximum of the power spectral density of each decaying sinusoid. The distributions are lopsided to higher frequencies as would be expected from fluctuations in the gate charge around our operating point at the sweet spot. The dashed line is the expected distribution assuming the same $1/f$ charge noise as in (c).

by a free evolution period of length Δt, followed by a readout measurement. We average the data in the same manner as "method A" in Ref. 21. A sequence of 700 Ramsey pulses with varying Δt, completing a full Ramsey fringe, is applied to the sample and then repeated and averaged to attain the required signal to noise ratio. An example of the resulting Ramsey fringes is shown in Fig. 5(b). By fitting to an exponentially decaying sinusoid, we extract an individual measurement of T_2 and Ramsey fringe frequency. The average frequency of Ramsey fringes is well fitted by the absolute value of the detuning $|\nu_s-\nu_{01}|$, yielding a precise measurement of $\nu_{01}=14.346$ GHz. We follow the time evolution of T_2 and ν_{01} by recording a Ramsey fringe every 0.35 s [Fig. 5(a)]. We observe stochastic fluctuations of T_2 with an asymmetric bell shaped distribution peaking around 600 ns, with a long tail extending down to 150 ns [Fig. 5(c)]. If we would average over the 3000 above Ramsey traces (17.5 nm period), we would measure an average T_2 which converges to 500 ns, similar to the first Saclay result[2] obtained with a qubit with a similar E_J/E_{CP}. Note that a Hahn spin echo sequence compensates for decoherence due to low frequency variations of the qubit transition frequency.[22] However, we intentionally perform the standard Ramsey fringe protocol as a manner of studying these low frequency fluctuations and determining their source. The T_2 fluctuations are correlated with fluctuations in the Ramsey frequency, which only fluctuates toward higher frequencies, giving lopsided distributions, as shown on Fig. 5(d). At the sweet spot where we are working, variations in gate charge necessarily increase the transition frequency, whereas variations in flux decrease it. Variations in critical current would supposedly keep the distribution of frequencies more symmetric. We can therefore conclude that charge noise, not flux noise, is the dominant source of decoherence in our sample. Furthermore, if we suppose that the charge noise is Gaussian with a spectral density that has the usually invoked $1/f$ form[23] given by $S_q(\omega)=\alpha^2/|\omega|$, we can check if our data can be explained by this model. This was carried out by directly numerically simulating the corresponding variations in transition frequency and calculating the Ramsey signal in the conditions of the experiment. The distributions of both the extracted T_2 and ν_{Ramsey} are shown by the dashed lines in Figs. 5(c) and 5(d). We obtain good agreement with the data for a noise amplitude of $\alpha=1.9\times10^{-3}e$, agreeing with the range of previously measured values of this noise intensity parameter.[9,12] To reduce sensitivity to this charge noise, we can make the energy levels of the qubit almost insensitive to charge by increasing E_J/E_{CP}. This is achieved by increasing the areas of the junctions in the SCPB or by increasing the capacitance of the island to ground.[24,25] An E_J/E_{CP} of 8 could give a T_2 in the millisecond range and hence this device would be T_1 limited.

CONCLUSION

We have successfully implemented an improved version of the bifurcation amplifier based on an on-chip CPW resonator as a readout for the quantronium qubit. It offers ease of fabrication and a larger range of operating parameters (ω_0, Q) compared to the original JBA implementation.[8] Using this readout which captures in real time the fluctuations

in qubit parameters, we have demonstrated that the main source of decoherence in our sample is charge noise. By using a larger E_J/E_{CP}, we could reduce the curvature with gate charge of the levels of the Cooper pair box and we should be able to reduce the charge noise induced decoherence. Furthermore, the CBA geometry is particularly well adapted to the multiplexing of the simultaneous readout of several qubits. We have started in this direction by successfully measuring the bifurcation of five CBAs with only one input and one output line. This configuration offers a path for scaling up of superconducting circuits up to several tens of qubits. Furthermore, cavity bifurcation amplification has further applications outside the realm of superconducting qubits, particularly in the measurement of any phenomenon that can be coupled to the Josephson energy.

ACKNOWLEDGMENTS

The authors would like to thank D. Prober, D. Esteve, S. Fissette, J. M. Gambetta, S. Girvin, and D. Vion for useful discussions and assistance. This work was supported by NSA through ARO Grant No. W911NF-05-01-0365, the Keck foundation, and the NSF through Grant No. DMR-032-5580. L.F. acknowledges partial support from CNR-Istituto di Cibernetica, Pozzuoli, Italy. M. H. D. acknowledges partial support from College de France.

[1] M. H. Devoret and J. M. Martinis, Quantum Inf. Process. **3**, 1 (2004); M. H. Devoret, in *Quantum Fluctuations*, edited by S. Reynaud, E. Giacobino, and J. Zinn-Justin (Elsevier, Amsterdam, 1997), p. 351.

[2] D. Vion, A. Aassime, A. Cottet, P. Joyez, H. Pothier, C. Urbina, D. Esteve, and M. H. Devoret, Science **296**, 866 (2002).

[3] P. Bertet, I. Chiorescu, G. Burkard, K. Semba, C. J. P. M. Harmans, D. P. DiVincenzo, and J. E. Mooij, Phys. Rev. Lett. **95**, 257002 (2005).

[4] T. Kutsuzawa, H. Tanaka, S. Saito, H. Nakano, K. Semba, and H. Takayanagi, Appl. Phys. Lett. **87**, 073501 (2005).

[5] B. L. T. Plourde, T. L. Robertson, P. A. Reichardt, T. Hime, S. Linzen, C.-E. Wu, and J. Clarke, Phys. Rev. B **72**, 060506(R) (2005).

[6] A. Wallraff, D. I. Schuster, A. Blais, L. Frunzio, R.-S. Huang, J. Majer, S. Kumar, S. M. Girvin, and R. J. Schoelkopf, Nature (London) **431**, 162 (2004).

[7] R. McDermott, R. W. Simmonds, M. Steffen, K. B. Cooper, K. Cicak, K. D. Osborn, Seongshik Oh, D. P. Pappas, and J. M. Martinis, Science **307**, 1299 (2005).

[8] I. Siddiqi, R. Vijay, M. Metcalfe, E. Boaknin, L. Frunzio, R. J. Schoelkopf, and M. H. Devoret, Phys. Rev. B **73**, 054510 (2006).

[9] G. Ithier *et al.*, Phys. Rev. B **72**, 134519 (2005).

[10] V. E. Manucharyan, E. Boaknin, M. Metcalfe, R. Vijay, I. Siddiqi, and M. H. Devoret, Phys. Rev. B **76**, 014524 (2007).

[11] E. Boaknin, V. E. Manucharyan, S. Fissette, M. Metcalfe, L. Frunzio, R. Vijay, I. Siddiqi, A. Wallraff, R. J. Schoelkopf, and M. H. Devoret, arXiv:cond-mat/0702445 (unpublished).

[12] Y. Nakamura, Yu. A. Pashkin, T. Yamamoto, and J. S. Tsai, Phys. Rev. Lett. **88**, 047901 (2002).

[13] I. Siddiqi, R. Vijay, F. Pierre, C. M. Wilson, M. Metcalfe, C. Rigetti, L. Frunzio, and M. H. Devoret, Phys. Rev. Lett. **93**, 207002 (2004).

[14] I. Siddiqi *et al.*, Phys. Rev. Lett. **94**, 027005 (2005).

[15] L. Frunzio, A. Wallraff, D. Schuster, J. Majer, and R. J. Schoelkopf, IEEE Trans. Appl. Supercond. **15**, 860 (2005).

[16] G. J. Dolan, Appl. Phys. Lett. **31**, 337 (1977).

[17] A. Cottet, Ph.D. thesis, University P. and M. Curie Paris 2002.

[18] I. I. Rabi, Phys. Rev. **51**, 652 (1937).

[19] N. F. Ramsey, Phys. Rev. **78**, 695 (1950).

[20] R. W. Simmonds, K. M. Lang, D. A. Hite, S. Nam, D. P. Pappas, and J. M. Martinis, Phys. Rev. Lett. **93**, 077003 (2004).

[21] D. J. Van Harlingen, T. L. Robertson, B. L. T. Plourde, P. A. Reichardt, T. A. Crane, and John Clarke, Phys. Rev. B **70**, 064517 (2004).

[22] E. Collin, G. Ithier, A. Aassime, P. Joyez, D. Vion, and D. Esteve, Phys. Rev. Lett. **93**, 157005 (2004).

[23] A. B. Zorin, F. J. Ahlers, J. Niemeyer, T. Weimann, H. Wolf, V. A. Krupenin, and S. V. Lotkhov, Phys. Rev. B **53**, 13682 (1996).

[24] D. I. Schuster *et al.* Nature (London) **445**, 515 (2007).

[25] Jens Koch, Terri M. Yu, Jay Gambetta, A. A. Houck, D. I. Schuster, J. Majer, A. Blais, M. H. Devoret, S. M. Girvin, and R. J. Schoelkopf, arXiv:cond-mat/0703002 Phys Rev. A (to be published).